



ELSEVIER

Contents lists available at ScienceDirect

Planetary and Space Science

journal homepage: www.elsevier.com/locate/pss739 observed NEAs and new 2–4 m survey statistics within the EURONEAR network [☆]

O. Vaduvescu ^{a,b,c,*}, M. Birlan ^b, A. Tudorica ^{d,e}, M. Popescu ^{b,f,h}, F. Colas ^b, D.J. Asher ^j,
 A. Sonka ^{g,h}, O. Suciuc ^{i,k}, D. Lacatus ^{l,m,p}, A. Paraschiv ^{l,m,p}, T. Badescu ⁿ, O. Tercu ^{o,p},
 A. Dumitriu ^{o,p}, A. Chirila ^{o,p}, B. Stecklum ^q, J. Licandro ^{c,r}, A. Nedelcu ^{b,f}, E. Turcu ^s,
 F. Vachier ^b, L. Beauvalet ^b, F. Taris ^b, L. Bouquillon ^b, F. Pozo Nunez ^t, J.P. Colque Saavedra ^u,
 E. Unda-Sanzana ^u, M. Karami ^{a,v,w}, H.G. Khosroshahi ^v, R. Toma ^{j,k}, H. Ledo ^{a,z}, A. Tyndall ^{x,a},
 L. Patrick ^{a,y}, D. Föhning ^{a,aa}, D. Muelheims ⁿ, G. Enzian ⁿ, D. Klaes ⁿ, D. Lenz ⁿ, P. Mählberg ⁿ,
 Y. Ordenes ⁿ, K. Sendlinger ⁿ

^a Isaac Newton Group of Telescopes (ING), Apartado de Correos 321, E-38700 Santa Cruz de la Palma, Canary Islands, Spain

^b IMCCE, Observatoire de Paris, 77 Avenue Denfert-Rochereau, 75014 Paris Cedex, France

^c Instituto de Astrofísica de Canarias (IAC), C/Vía Láctea s/n, 38205 La Laguna, Spain

^d Bonn Cologne Graduate School of Physics and Astronomy, Germany

^e Argelander-Institut für Astronomie, Universität Bonn, Auf dem Hügel 71, D-53121 Bonn, Germany

^f The Astronomical Institute of the Romanian Academy, Cutitul de Argint 5, 040557 Bucharest, Romania

^g The Astronomical Observatory "Admiral Vasile Urseanu", B-dul Lascar Catargiu 21, Bucharest, Romania

^h Bucharest Astroclub, B-dul Lascar Catargiu 21, sect 1, Bucharest, Romania

ⁱ Babes-Bolyai University, Faculty of Mathematics and Informatics, 400084 Cluj-Napoca, Romania

^j Armagh Observatory, College Hill, Armagh BT61 9DG, Northern Ireland, United Kingdom

^k Romanian Society for Meteors and Astronomy (SARM), CP 14 OP 1, 130170 Targoviste, Romania

^l Research Center for Atomic Physics and Astrophysics, Faculty of Physics, University of Bucharest, Atomistilor 405, CP Mg-11, 077125 Magurele, Ilfov, Romania

^m Institute of Geodynamics Sabba S. Stefanescu, Jean-Louis Calderon 19-21, Bucharest RO-020032, Romania

ⁿ Rheinische-Friedrich-Wilhelms Universität Bonn, Argelander-Institut für Astronomie, Auf dem Hügel 71, D-53121 Bonn, Germany

^o Galati Astronomical Observatory of the Natural Sciences Museum Complex, Str. Regiment 11-Siret, no 6A, 800340 Galati, Romania

^p Calin Popovici Astronomy Club, Str. Regiment 11-Siret, no 6A, 800340 Galati, Romania

^q Thüringer Landessternwarte Tautenburg, Sternwarte 5, D-07778 Tautenburg, Germany

^r Departamento de Astrofísica, Universidad de La Laguna, E-38205 La Laguna, Tenerife, Spain

^s The Astronomical Observatory of "Stefan cel Mare" University of Suceava, Str. Universitatii 13, 720229 Suceava, Romania

^t Instituto de Astronomia, Universidad Católica del Norte, Avenida Angamos 0610, Antofagasta, Chile

^u Unidad de Astronomia, Universidad de Antofagasta, Avda. Angamos 601, 1270300 Antofagasta, Chile

^v School of Astronomy, Institute for Research in Fundamental Sciences (IPM), PO Box 19395-5531, Tehran, Iran

^w Sharif University of Technology, Azadi Ave., PO Box 11365-11155, Tehran, Iran

^x Jodrell Bank Centre for Astrophysics, School of Physics and Astronomy, University of Manchester, M13 9PL, United Kingdom

^y Department of Physics and Astronomy, University of Sheffield, Sheffield S3 7RH, United Kingdom

^z Centre for Astrophysics Research, University of Hertfordshire, College Lane, Hatfield AL10 9AB, United Kingdom

^{aa} Department of Physics, Centre for Advanced Instrumentation, University of Durham, South Road, Durham DH1 3LE, United Kingdom

ARTICLE INFO

Article history:

Received 12 December 2012

Received in revised form

7 May 2013

Accepted 27 June 2013

Available online 8 July 2013

ABSTRACT

We report follow-up observations of 477 program Near-Earth Asteroids (NEAs) using nine telescopes of the EURONEAR network having apertures between 0.3 and 4.2 m. Adding these NEAs to our previous results we now count 739 program NEAs followed-up by the EURONEAR network since 2006. The targets were selected using EURONEAR planning tools focusing on high priority objects. Analyzing the resulting orbital improvements suggests astrometric follow-up is most important days to weeks after discovery, with recovery at a new

[☆]Based on observations taken with the following telescopes: Blanco 4 m in Chile, INT 2.5 m and WHT 4.2 m in La Palma, OHP 1.2 m and Pic du Midi 1 m in France, Tautenburg 2 m and Bonn AIfA 0.5 m in Germany, Galati 0.4 m and Urseanu 0.3 m in Romania.

* Corresponding author at: Isaac Newton Group of Telescopes (ING), Apartado de Correos 321, E-38700 Santa Cruz de la Palma, Canary Islands, Spain.

Tel.: +34 92 2425461.

E-mail addresses: ovidiu.vaduvescu@gmail.com,
ovidiv@ing.iac.es (O. Vaduvescu).

Keywords:

Minor planets
Near Earth Asteroids
Main belt asteroids
Astrometry and orbits
Follow-up and discovery
Survey statistics

opposition also valuable. Additionally we observed 40 survey fields spanning three nights covering 11 square degrees near opposition, using the Wide Field Camera on the 2.5 m Isaac Newton Telescope (INT), resulting in 104 discovered main belt asteroids (MBAs) and another 626 unknown one-night objects. These fields, plus program NEA fields from the INT and from the wide field MOSAIC II camera on the Blanco 4 m telescope, generated around 12000 observations of 2000 minor planets (mostly MBAs) observed in 34 square degrees. We identify Near Earth Object (NEO) candidates among the unknown (single night) objects using three selection criteria. Testing these criteria on the (known) program NEAs shows that the best selection method is our $\epsilon-\mu$ model which checks solar elongation and sky motion and the MPC's NEO rating tool. Our new data show that on average 0.5 NEO candidates per square degree should be observable in a 2 m-class survey (in agreement with past results), while an average of 2.7 NEO candidates per square degree should be observable in a 4 m-class survey (although our Blanco statistics were affected by clouds). At opposition just over 100 MBAs (1.6 unknown to every 1 known) per square degree are detectable to $R=22$ in a 2 m survey based on the INT data (in accordance with other results), while our two best ecliptic Blanco fields away from opposition lead to 135 MBAs (2 unknown to every 1 known) to $R=23$.

© 2013 Elsevier Ltd. All rights reserved.

1. Introduction

Since Ceres was found by Piazzi in 1801, the discovery rate of Main Belt Asteroids (MBAs) has increased, to the point where the IAU Minor Planet Center (MPC) has now cataloged over 600,000 minor planets (Minor Planet Center, 2012a). Near Earth Asteroids (NEAs), defined as minor planets with perihelion distance $q \leq 1.3$ AU and aphelion distance $Q \geq 0.983$ AU (Morbidelli and et al., 2002), represent an important Solar System population: their main formation mechanisms include migration of MBAs due to resonances, especially 3:1 mean-motion with Jupiter and ν_6 with Saturn (Farinella et al., 1993), possibly combined with the Yarkovsky/YORP effects (Bottke et al., 2006). There are more than 9200 known NEAs today (Minor Planet Center, 2012a).

Potentially Hazardous Asteroids (PHAs) are defined as a sub-class of NEAs having minimum orbital intersection distance $MOID \leq 0.05$ AU and absolute magnitude $H \leq 22$ (Bowell and Muinonen, 1994). We know today more than 1300 PHAs (Minor Planet Center, 2012a). Virtual Impactors (VIs) are NEAs whose future Earth impact probability is non-zero according to the actual orbital uncertainty (Milani and Gronchi, 2009). There are about 420 and 350 VIs listed in the NASA JPL Sentry Risk Table (NASA JPL, 2012) and NEODyS Risk List (NEODyS, 2012), respectively.

There is a continual need to observe asteroids in order to study their orbits and, for NEAs, to catalog future approaches to Earth. New astrometry improves the orbital quality which would otherwise be degraded by effects including close planetary approaches and non-gravitational effects (Yarkovsky, YORP).

The European Near Earth Asteroid Research (EURONEAR) was initiated in 2005 in Paris in order to bring some European contribution to the NEA research using existing telescopes and hopefully some automated dedicated facilities (EURONEAR, 2012a). Lacking dedicated funding, during recent years mostly volunteering students and amateur astronomers directed by a few researchers reduced the data in near real time (few hours or days after acquisition), some of them participating in observing runs. Vaduvescu et al. (2008) introduced EURONEAR and first observations obtained at Pic du Midi in 2006, followed by Birlan et al. (2010a) who described the first 160 observed NEAs using nine telescopes available to the EURONEAR network during the first four years. Vaduvescu et al. (2011) presented some MBA and NEA statistics based on three runs using large field 1–2 m facilities (Swope 1 m, ESO/MPG 2.2 m and INT 2.5 m).

In this paper we present new NEA recovery and follow-up observations using six professional and three educational-amateur telescopes available to the EURONEAR network during the last two years. Adding these observations, the total number of observed

NEAs within the EURONEAR network reaches 739 objects (October 2012). Thanks to two observing runs and a few discretionary time hours awarded to use the large field imaging cameras of the 2.5 m Isaac Newton Telescope (INT) and Blanco 4 m telescope, in a team comprised mostly of students and amateur astronomers we obtained and carefully analyzed 572 CCD fields covering 34 square degrees, visually scanning, measuring and reporting around 12 thousand positions of more than two thousand asteroids. We have then used the data obtained with 2–4 m telescopes to derive MBA and NEA statistics going beyond our previous results based on data obtained with 1–2 m facilities (Vaduvescu et al., 2011).

Section 2 describes our observations. In Section 3 we compile the results, including the classification into observed NEAs, known MBAs and unknown objects. In Section 4 we discuss these results, focusing on the distribution of the known and unknown MBAs and NEAs; we compare the INT and Blanco facilities and present statistics for the use of 2 m and 4 m class surveys. Conclusions and two future projects are presented in Section 5.

2. Observations and data reduction

To distinguish between targeted and new candidate NEAs, we define as *program NEA* any Near Earth Asteroid (NEA, PHA or VI) programmed for follow-up within the EURONEAR network. To plan our runs and select program NEAs given an observing place and date, we used two planning tools (EURONEAR, 2012b) which target the newly discovered objects from the Spaceguard priority list (Spaceguard System, 2012) and the NEA bright and faint recovery opportunity lists maintained by the Minor Planet Center (Minor Planet Center, 2012a). More information about these planning tools can be found in Vaduvescu et al. (2011).

Ten cameras mounted on nine telescopes were used between January 2009 and June 2012. In Table 1 we list specifications of each facility. We present each observing node and results next. For all observing sites and runs except TLS we used Astrometrica (Raab, 2012) to identify program NEAs and other moving sources, using its field recognition, image registering and blinking capabilities, by visually scanning, measuring and reporting the observed fields in near real time (few hours or days after the runs). For relatively sparse observations and small sky area covered, Astrometrica has been proven an excellent team capability for use by students and amateurs. Moreover, for limited amounts of data, the human eye and brain have been better for moving object detection, reaching lower S/N detection versus automated pipelines (see for example Vaduvescu et al., 2011 for some references and comparison).

Table 1

Telescopes and detectors used for follow-up, recovery and securing orbits of NEAs. The columns give the observatory, telescope aperture (m), CCD camera, number of CCDs and individual size in pixels, field of view and pixel scale.

Telescope	Aperture	Camera	CCDs and Pixels	FOV (')	Scale ("/pix)
ORM INT	2.5	WFC	4 × (2048 × 4096)	34 × 34 L	0.333
ORM WHT	4.2	ACAM	2048 × 4096	8 diam	0.254
CTIO Blanco	4.0	MOSAIC II	8 × (2048 × 4096)	36 × 36	0.27
Pic du Midi (b)	1.05	iKon-L Andor	2048 × 2048	7.5 × 7.5	0.22
Pic du Midi (c)	1.05	Atik 383L+	3326 × 2504	7.8 × 5.8	0.14
Haute Provence	1.20	TK1024	1024 × 1024	11.7 × 11.7	0.685
TLR Tautenburg	2/1.34	SITe	2048 × 2048	42 × 42	1.23
Bonn/AlfA	0.50	SBIG-STL 6303E	3072 × 2048	23.0 × 15.4	0.45
Galati	0.40	SBIG STL-6303E	3072 × 2048	29.8 × 19.9	0.58
Urseanu	0.30	TC273-home made	640 × 500	21.6 × 16.9	2.30

2.1. INT observing runs

We used the 2.5 m Isaac Newton Telescope (INT) owned by the Isaac Newton Group (ING) at Roque de Los Muchachos Observatory (ORM) in La Palma. Four nights were awarded by the Spanish Time Allocation Committee (CAT, 25–28 February 2012, proposal number C6, PI: O. Vaduvescu) and approximately 10 h were used in total during four service/discretionary ING nights

(S/D) in 2011.

At the prime focus of the INT we used the Wide Field Camera (WFC) which consists of four CCDs $2K \times 4K$ pixels each covering an L-shaped $34' \times 34'$ with a pixel scale of $0.33"/\text{pix}$. All frames were observed with 2×2 binning ($0.66"/\text{pix}$) to decrease the readout time, except for the December 2011 run which was operated without binning. During three of the S/D nights (except for December 2011 run) we tracked the observed fields at half the NEA proper motion, while for the remaining runs we tracked fields at normal sidereal rate. The filling factor of the WFC (defined as the ratio of the active area over total sky subtended camera area) is 0.86. We used an R filter for all runs.¹

The CAT time was dark, and the weather was good during three nights, except for the first 3 h during the second night and the third night when we closed due to humidity. The typical seeing at the INT was $\sim 1.5''$. For data reduction we used THELI (Erben et al., 2005) to correct the field distortion in the prime focus of the INT, then using Astrometrica with a fit order 1–2 and USNO-B1 or NOMAD (thus UCAC2) catalogs.

Besides the program NEAs (listed in Table A1 in the Appendix), during three clear nights at the INT in February 2012 (the first, second and fourth of our run) we undertook an MBA mini-survey around opposition, covering in total 40 WFC fields (five successive images of the same field) during 12 h total time. The pointing grid of the MBA mini-survey was optimized in order to recover most new MBAs observed on previous night(s), assuming a daily apparent motion of $17'$ westward along the ecliptic (based on $0.7''/\text{min}$ average speed). During the first night we observed 10 arbitrarily chosen WFC fields close to opposition in the ecliptic. During the second night we observed the same 10 WFC fields shifted by -1 min in α and $+8'$ in δ . During the fourth night we observed a pair of fields shifted by -2 min in α and $+16'$ and $-1'$ in δ with respect to the second night. During the short time available for this mini-survey, this pointing grid allowed us to recover many objects appearing in previous nights in the WFC fields and maximize the number of MBA discoveries.

Due to the large WFC field and INT aperture, we measured and identified all moving sources detected visually via blinking in all

observed fields in all INT runs, reporting all known and new objects visible up to apparent magnitude $R \sim 22$. In total, at the INT we observed 87 WFC fields covering ~ 24 square degrees (including 40 WFC fields covering 11 square degrees in our opposition mini-survey). We followed or recovered 33 program NEAs (including 4 PHAs and 1 VI), making the INT-WFC one of the most productive EURONEAR facilities for recovery and survey work (NEAs and MBAs). In Section 4.3 we use the INT findings for MBA and NEA statistics.

2.2. Blanco observing run

The first EURONEAR run using a 4 m telescope was awarded by the Chilean Time Allocation Committee for 3–4 June 2011 (proposal number 0646, PI: E. Unda-Sanzana) to use the Victor Blanco 4 m telescope at Cerro Tololo Inter-American Observatory (CTIO) in Chile. At the prime focus $F/2.9$ of the telescope we employed the MOSAIC II camera which consists of a 2×4 mosaic of CCDs $2K \times 4K$ pixels each covering a total field of view of $36' \times 36'$ with a pixel scale of $0.27''/\text{pix}$. To minimize the readout time and FTP data transfer, we used 2×2 binning (binned pixel size $0.54''$). We used an R filter for the entire Blanco run. The filling factor of the MOSAIC II camera is 0.98. We used normal sidereal tracking for all fields.

The time was dark, with only the first night clear and its first 3 h affected by clouds, resulting in no NEA recovered in the first nine program NEA fields. The second night had complete cloud cover, one day before a big snow storm which hit Cerro Tololo. During the first night we recovered 12 program NEAs (including 1 VI and 9 PHAs) plus two other NEAs falling by chance in the observed fields (1 PHA). The typical seeing was $\sim 1''$.

For data reduction we used the USNO-B1 catalog and no field correction due to lack of time to fit THELI to work in binning mode with MOSAIC II. First, we reduced data allowing the high field distortion to be accommodated by a fit order 3 in Astrometrica. Then, the MPC advised us about some errors (Williams, private communication) which we traced to the high field distortion of the prime focus camera, thus we restricted Astrometrica to a fit order 2 which allowed better astrometry.

Besides NEAs (Table A1), we identified and measured all moving sources in all observed fields (except for four fields falling in the Milky Way), reporting all known and new objects visible up to $R \sim 24$ mag. Using Blanco during one night, we observed in total 28 MOSAIC II fields covering in total 10 square degrees. In Section 4.3 we use Blanco data to derive some MBA and NEA statistics.

2.3. WHT observing runs

A few observations to recover some NEAs were conducted during twilight or combined with some technical tasks during four service or discretionary (S/D) nights in 2011, using the William

¹ Historically we used R filter for most of our EURONEAR runs in order to minimize moonlight, artificial light pollution and also for photometric consistency.

Herschel 4.2 m Telescope (WHT) of the ING located at ORM. Additionally, during other two service nights in 2011 we observed for photometry the OSIRIX-Rex target (the VI (101 955) 1999 RQ36) under the program SW2011a31 (PI: J. Licandro), for about 8 h in total. In total using the WHT, we observed 11 program NEAs (including 4 PHAs and 1 VI). We used guiding only for the photometry runs of (101 955), tracking at normal sidereal rate for the other fields.

At the Cassegrain $F/11$ focus we used the ACAM camera which consists of one CCD with $2K \times 4K$ pixels covering a field of view of $8'$ diameter with a pixel scale of $0.25''/\text{pix}$. We used R filters for all WHT runs. The weather was mostly good, with WHT ACAM typical seeing around $1''$. In Table A1 we list the program NEAs observed with WHT.

For data reduction we used IRAF for typical flat and bias corrections and Astrometrica with a fit order 1–2 (sufficient for the Cassegrain instrument), using mostly USNO-B1, UCAC3 or UCAC4 depending on the star density in the observed small ACAM field.

2.4. TLS observing runs

Türinger Landessternwarte Observatory (TLS) located in Tautenburg, Germany, joined the EURONEAR network in 2009, starting regular NEA observations in 2011 using the Alfred Jensch 2 m telescope (1.34 m Schmidt corrector plate). At the Schmidt $F/4$ focus of the TLS telescope is a SITe CCD $2k \times 2k$ camera, covering a large field of view $42' \times 42'$ with a pixel scale of $1.23''/\text{pix}$.

During 39 nights in September 2011, March, and May 2012, a total of 38 NEAs, mostly very recently discovered objects, were observed (Table A1). The median seeing in Tautenburg is $\sim 2''$ and the R filter was used for all runs. The TLS pipeline which includes run planning and data reduction is complete, and few runs are planned in the near future.

Astrometry and field correction are resolved using *Astrometry.net* (Lang et al., 2010) with the GSC 2.3 catalog. The exposure time used at TLS was a standard 180 s for all NEAs. The observing technique and data reduction method are a novelty in EURONEAR, so we briefly present this here. Depending on the magnitude and proper motion of the object, a few frames are taken with same exposure time in normal sidereal auto-guiding, thus the asteroid becomes visible as a trail. After basic correction of bias and flat field, field distortion and astrometry are resolved with *astrometry.net*, using second order SIP polynomials to account for field distortion. The median co-added image is created by registering all images on the center of the NEA trail given the shifts calculated from the ephemeris. Finally, the NEA trail will be deconvolved

using a PSF artificial trail (length and direction from motion, width from stellar PSF) to model the centrally peaked elongated brightness distribution of the object. Finally, the co-added trail is fitted by an elliptical Gaussian to come up with object coordinates and errors.

Fig. 1 shows the case of the extremely newly discovered (one day) fast NEA 2012 FP35 moving with $\mu = 100.5''/\text{min}$. The left image is the result of adding two registered frames, resulting in two observed trails which do not exactly superimpose because of the large uncertainty in the orbit (e.g. position and proper motion). The predicted position is indicated by the green circle while the observed one (the result of the fit) is marked by the red circle. The right image represents the recovered deconvolved image where the stars become elongated.

2.5. OHP observing runs

Two observing runs (10 nights in total) were awarded in 20–24 April 2010 and 15–19 November 2010 by the Local Time Allocation Committee using the 1.2 m telescope (T120) at Haute de Provence Observatory (OHP) in France.

The Newtonian $F/6$ T120 telescope hosted the TK 1024 AB camera equipped with a $1k \times 1k$ CCD covering a $11.7' \times 11.7'$ field of view with a pixel scale of $0.68''/\text{pix}$. The median seeing at OHP was about $2.5''$. The R filter was used for both runs and normal sidereal tracking. For data reduction we used Astrometrica with fit order 1 and USNO-B1 catalog to provide enough stars for the relatively small and shallow observed fields.

Past (pre-2010) OHP observations were reported by Birlan et al. (2010a). In total during the 2010 runs we observed 36 program NEAs (including 8 PHAs; Table A1).

2.6. Pic du Midi observing runs

Two observing runs (10 nights in total) were awarded in 1–4 March 2011 and 17–24 November 2011 by the *Station de Planéologie des Pyrenees* managed by *Observatoire de Paris* and *Observatoire Midi Pyrenees* at Pic du Midi Observatory, France. For both runs the T1m 1.05 m telescope was used.

For the first run, at the Cassegrain $F/12.1$ reduced focus we employed the iKon-L Andor camera with a $2k \times 2k$ E2V chip with pixel scale $0.22''/\text{pix}$. To reduce the noise we used 2×2 binning, so a pixel size of $0.44''$ with a field of view of $7.5' \times 7.5'$. For the second run at the Cassegrain $F/7.6$ reduced focus we employed the Atik 383L+ camera with an 3326×2504 CCD Kodak KAF-8300 chip with pixel scale $0.14''/\text{pix}$. We used 3×3 binning, so a pixel size of $0.42''$ with a field of view of $7.8' \times 5.8'$. For both runs we

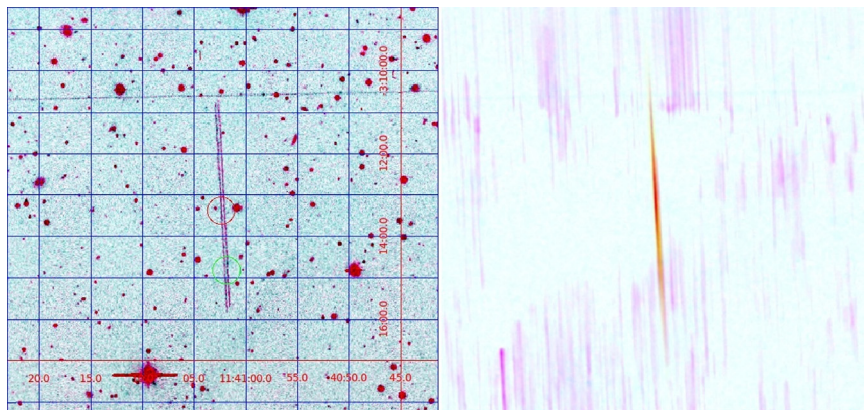


Fig. 1. The very fast NEA 2012 FP35 observed at TLS using the trail deconvolution reduction method. On the left side we present the observed image obtained by shifting and stacking the two individual frames. The right side presents the result after deconvolution showing the data (magenta) and the fit (dark yellow). (For interpretation of the references to color in this figure caption, the reader is referred to the web version of this article.)

used a clear filter from Astronomik equivalent to $B + V + R$ with bandpass from 390 nm to 680 nm, tracking at half the proper motion of observed NEAs.

Typical seeing at Pic du Midi was about 1.5". The weather was good and the Moon was mostly dark. For the data reduction we used Astrometrica with fit order 1, enough for the Cassegrain field, and USNO-B1 and NOMAD catalogs, depending on available star density in the fields.

Past EURONEAR Pic du Midi observations were reported in Vaduvescu et al. (2008) and Birlan et al. (2010a). During the two Pic du Midi 2011 runs, 34 NEAs were observed (including 5 PHAs and 1 VI; Table A1).

2.7. Bonn/Alfa observing runs

The Argelander Institute for Astronomy (Alfa) owns a 0.5 m telescope hosting at its Cassegrain $F/9$ focus an SBIG-STL 6303E CCD camera (3072×2048 pixels, scale 0.45"/pixel). The typical seeing there is about 3" and the light pollution is quite high (naked-eye mag 4 at zenith) allowing mag 19 to be reached only after stacking a few short exposed images (using Astrometrica's "track and stack" capability). We observed with 2×2 binning using V and R filters, tracking all fields at normal sidereal rate. We used Astrometrica with UCAC3 and USNO-B2 catalogs and no field correction in the Cassegrain field.

The MPC code of the Bonn/Alfa observatory C60 was obtained by A. Tudorica (MSc student there) who joined the Bonn/Alfa node to the EURONEAR network in 2011. During 25 nights between September 2011 and May 2012, we observed 60 NEAs (of which 15 PHAs) and reported 830 positions.

2.8. Galati observing runs

The public Astronomical Observatory of the Natural Sciences Museum Complex in the city of Galati, Romania, was found thanks to the efforts of O. Tercu, the actual observatory coordinator, based on funding from the county of Galati (*Consiliul Judetean Galati*), plus other funding from the E.U. and some local sponsorship. The observatory joined the EURONEAR network in 2010 and obtained the MPC code C73 in 2011. Supported by a small but enthusiastic team of amateurs in the local astronomy club "Calin Popovici", Galati observatory includes NEAs as one of their main priorities for public outreach and education.

Among other smaller telescopes and instruments, the main telescope of Galati observatory is the ASA 0.4 m Ritchey-Chretien $F/8$ telescope endowed with an SBIG STL-6303E CCD with 3072×2048 pixels covering a relatively large field of view $29.8' \times 19.9'$ with pixel scale 0.58"/pix.

All NEA observations of Galati Observatory were performed using 2×2 binning (binned pixel size 1.16"/pix), due to the typical seeing of about 3". For all runs we used normal tracking at sidereal rate. For data reduction we used Astrometrica with UCAC3 catalog and a fit order 4 to correct the relatively distorted large field.

During 55 nights between September 2011 and May 2012 three people observed 223 NEAs (of which 40 PHAs and 4 VIs) and reported 2367 positions, becoming the most prolific EURONEAR site in terms of number of observed objects and NEA public outreach. Despite some city light pollution, the 40-cm telescope manages to reach limiting magnitude $V \sim 19$.

2.9. Urseanu observing runs

The public "Admiral Vasile Urseanu Observatory" in Bucharest, Romania, was found in 1910 by the navy admiral Vasile Urseanu who was also an amateur astronomer. The actual public meeting place of many visitors and host of the Bucharest

Astroclub, the observatory is owned by the Bucharest Museum of History. Thanks to the efforts of A. Sonka, in 2006 the observatory obtained its MPC code A92, becoming one of the first EURONEAR nodes.

The very small 0.3 m telescope (Meade LX200R) of the Urseanu Observatory is actually the smallest used by our network, being extensively used for public outreach there. At the Cassegrain $F/6.3$ field resides an inexpensive QHY6 CCD camera. The pixel scale is 2.30"/pix and the field is $21.6' \times 16.9'$. Typical seeing in the very light polluted capital Bucharest using this equipment is about 3" and the limiting magnitude is $V \sim 16$ ($V \sim 15$ for fast moving objects). For all runs we used sidereal tracking.

Past NEA observations from Urseanu Observatory were reported in Vaduvescu et al. (2008) and Birlan et al. (2010a). From November 2008 until May 2012 a total of 28 NEAs (including 9 PHAs and 1 VI) were observed and reported from this observatory.

3. Results

3.1. Program NEAs

A total of 477 program NEAs observed within the EURONEAR network between 2009 and May 2012 are reported in this paper. Of these, 166 were observed with six professional 1–4 m telescopes and 311 with three smaller (0.3–0.5 m) educational and public outreach telescopes. In the Appendix Table A1 we give the observing logs containing these objects observed with the above nine telescopes. In Fig. 2 we plot the O–C (observed minus calculated) residuals in α and δ for the program NEAs observed with each telescope.

The root mean square of the O–C residuals for our MPC published NEA datasets for each telescope are in the order: WHT 0.44", INT 0.46", Blanco 0.46", Bonn 0.56", Galati 0.57", Pic 0.81", OHP 0.85", Urseanu 1.05" and TLS 1.14".

Overall, small amateur-educational telescopes Bonn and Galati are performing very good astrometry, only slightly inferior by 0.1" than their much larger 2–4 m "colleagues" INT, Blanco and WHT which also benefit from much better weather conditions. Owing to less accurate catalogs used (USNO-B1 versus UCAC3) and possibly due to target selection (newly discovered versus new opposition objects) we observe that O–Cs of our two 1 m facilities OHP and Pic trail behind Bonn and Galati by about 0.3". Thus, the loss in astrometric precision is absolutely non-linear with the shortening of aperture, the most important factors favoring the contribution from small telescopes being better astrometric catalogs used (especially in the bright regime more accessible to small telescopes), a good SNR for both target and reference stars and the absence of complicated field distortion, all in line with recommendations of the IAU Working Group "Astrometry by Small Ground Based Telescopes".

At least two inhomogeneities can be spotted in the O–C plots in Fig. 2. First, the small vertical branch in the OHP plot is due to few OHP objects moving much faster in δ than in α , resulting in larger measurement errors and O–Cs in δ . Second, the WHT O–C centroid seems slightly displaced (by about 0.2") to the upper-right from the origin, which is explained by the known systematics of the mostly used USNO-B1 catalog due to the small ACAM field (a fact observed also by us previously, Birlan et al., 2010a).

3.1.1. MPC/MPEC publications

Adding the 477 observed NEAs to our previous work presented in Birlan et al. (2010a) and Vaduvescu et al. (2011), we report a total of 739 NEAs observed within the EURONEAR network during

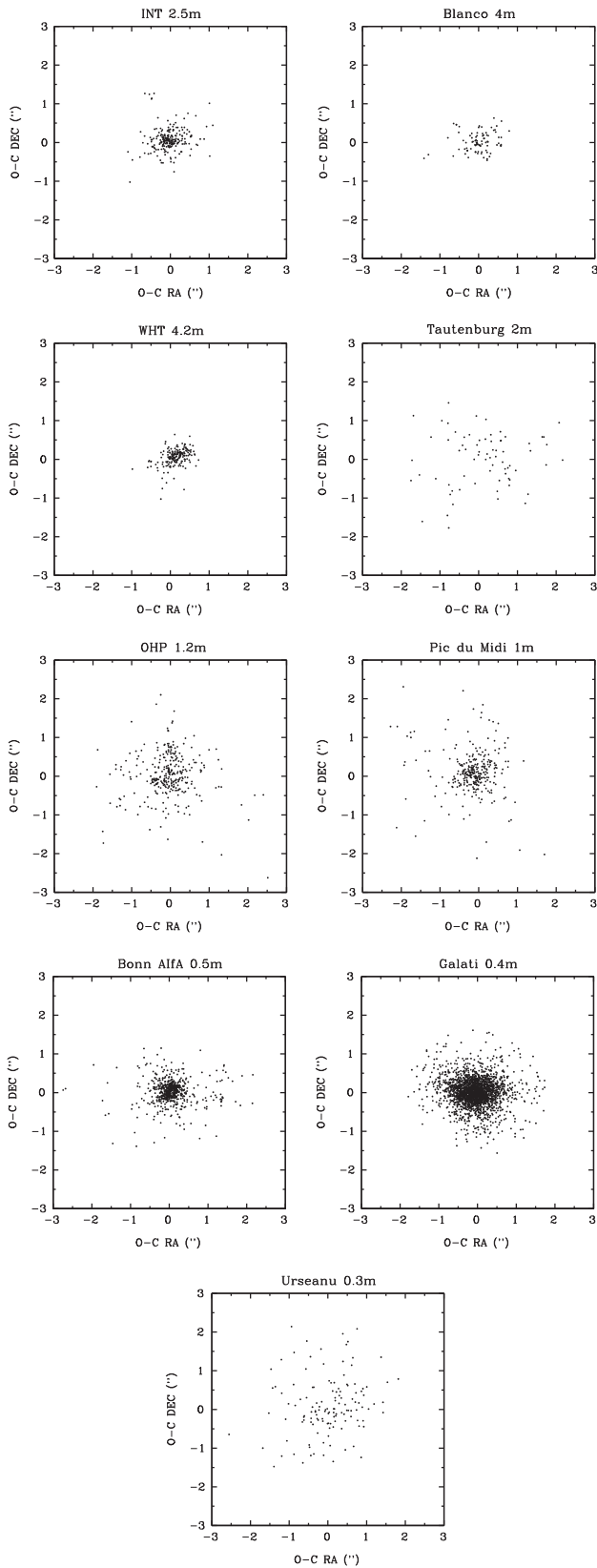


Fig. 2. O–C (observed minus calculated) residuals for program NEAs observed using the telescopes presented in this paper.

the last six years. The reduced data presented in this paper generated 98 MPC publications, comprising 69 Minor Planet Circulars (MPCs) and 29 Minor Planet Electronic Circulars (MPECs).

The Blanco run resulted in published data in the following eight MPC/MPEC publications: 74 496, 75 198, 75 623, 75 939, 76 865, 79 528 (Buie et al., 2011a,b,c,d,e, 2012), 76 441 and 77 265 (Elst et al., 2011a,b).

The INT runs resulted in published data in the following 11 MPC/MPEC publications: 76 443, 78 047, 78 437, 78 894, 79 221, 79 530 (Fitzsimmons et al., 2011a, 2012a,b,c,d,e), 75 625 (Holman et al., 2012), 79 787 and 2012-D82 (Vaduvescu et al., 2012a,b), 2012-E19 (Gajdos et al., 2012) and 2012-D102 (Bressi et al., 2012).

The WHT observations resulted in published data in the following eight MPC/MPEC publications: 74 148, 74 893, 75 207, 76 443, 77 266, 78 047 (Fitzsimmons et al., 2011a,b,c,d,e, 2012a), 75 625 (Holman et al., 2012) and 75 940 (Balam et al., 2011).

The OHP runs resulted in published data in the following six MPC/MPEC publications: 69 732, 72 456 (Arlot et al., 2010a,b), 70 198, 2010-W11, 2010-W12 and 2010-W13 (Birlan et al., 2010b,c,d,e).

The Pic du Midi runs resulted in published data in the following 17 MPC publications: 74 036, 77 173 (Cavadore et al., 2011a,b), 2011-E11, 2011-E12, 2011-E13, 2011-W29, 2011-W33 (Birlan et al., 2011a,b,c,d,e), 2011-E14 (Lehmann et al., 2011), 2011-E19 (Apitzsch et al., 2011), 2011-W25 (McMilan and et al., 2011), 2011-W12, 2011-W22, 2011-W27, 2011-W28, 2011-W44, 2011-W45 and 2011-W52 (Buzzi et al., 2011a,b,c,d,e,f,g).

Tautenburg runs resulted in published data in the following six MPC/MPEC publications: MPC 79 140, 79 473 (Borngen and Stecklum, 2012a,b), 79 746, 79 971 (Stecklum, 2012a,b), 2012-G45 and 2012-K07 (Stecklum et al., 2012a,b).

Bonn AIfA runs resulted in published data in the following nine MPC/MPEC publications: MPC 74 509, 79 224, 79 789, 80 000 (Tudorica, 2011, 2012a,b,c), 76 451 (Tudorica and Toma, 2011), 76 874, 78 902 (Tudorica and Badescu, 2011, 2012), 77 273 and 79 533 (Tudorica et al., 2012d,e).

The Galati runs resulted in published data in the following 17 MPC/MPEC publications: MPC 75 947, 76 451, 76 874, 77 273, 77 705, 78 053, 78 445, 78 902, 79 225, 79 533, 80 000 (Tercu and Dumitriu, 2011a,b,c,d, 2012a,b,c,d,e,f,g), 2012-B17 (Bacci et al., 2012), 2012-G45 (Stecklum et al., 2012a), 2012-H42 (Eglitis et al., 2012), 2012-H90 (Jaeger et al., 2012), 2012-J01 (Nishiyama and et al., 2011) and 2012-J34 (Christensen et al., 2012).

Finally, Urseanu runs resulted in published data in the following 16 MPC/MPEC publications: MPC 64 104, 65 048, 65 638, 65 928, 67 139, 67 404, 67 677, 698 17, 71 094, 72 053, 75 208, 75 447, 77 270, 77 702, 78 050 and 79 998 (Sonka, 2008, 2009a,b,c, d,e,f, 2010a,b,c, 2011a,b,c, 2012a,b,c).

3.1.2. Orbital improvement

We focus next on the NEAs recovered at a new opposition (29 objects marked by \star in Appendix Tables A1 and A2) and also on the NEAs followed-up soon after discovery—new objects whose arcs were either observed within the first day or prolonged by at least one day during the first month (82 objects marked by \bullet in Tables A1 and A2), studying the orbits of these 111 objects.

We use the software FIND_ORB (Gray, 2012) to assess the orbital improvement, by comparing the orbital elements fitted with observational data available before our runs (first line in Table A2) with those obtained adding our observations (second line in Table A2). We list in the table the semimajor axis a , eccentricity e , inclination i , longitude of ascending node Ω , argument of pericenter ω , mean anomaly M and minimum orbital intersection distance MOID.

Despite the importance of the recovery of NEAs at a new opposition which lengthens the observed arc by a few years, orbital elements of the NEAs recovered at a new opposition appear to be improved only slightly in absolute terms: standard deviations of the changes to elements (based on 25 pairs of orbits for

objects marked \star in Table A2) are $a \sim 10^{-4}$ AU, $e \sim 5 \times 10^{-5}$, $i \sim 10^{-3}$ deg, $\Omega \sim 10^{-3}$ deg, $\omega \sim 3 \times 10^{-3}$ deg, $M \sim 5 \times 10^{-2}$ deg, MOID $\sim 3 \times 10^{-5}$ AU and $\sigma \sim 0.02''$ (RMS of the fit).

Orbits of NEAs followed soon after discovery, as they are less well constrained a priori, naturally undergo larger changes to the elements following our observations, with standard deviations of $a \sim 10^{-1}$ AU, $e \sim 10^{-2}$, $i \sim 1$ deg, $\Omega \sim 1$ deg, $\omega \sim 1$ deg (all about 10^3 times more), $M \sim 7$ deg, MOID = 0.0151 AU and $\sigma \sim 0.06''$, based on 73 pairs of orbits representing objects observed with all telescopes marked \bullet in Table A2.

FIND_ORB additionally provides the option to calculate uncertainties in the orbits it determines, enabling us to assess the orbital quality both before and after our observations (as opposed to simply the change in the best estimate orbit due to our observations). We therefore calculated 1-sigma a , e and i uncertainties σ_a , σ_e and σ_i for Table A2 objects and can define orbital improvement as the ratio in the σ_a , σ_e or σ_i values before and after our EURONEAR observations. Fig. 3, and similar plots for e and i not shown, suggests that the orbital improvement is closely related to the increase in time interval spanned by the observations. This can be quantified by fitting log of orbital improvement to log of proportional increase in timespan. The formal linear regression results were

$$\begin{aligned} \log(\sigma_a \text{ ratio}) &= (1.35 \pm 0.22)\log T + (0.20 \pm 0.15), \\ \log(\sigma_e \text{ ratio}) &= (0.81 \pm 0.19)\log T + (0.26 \pm 0.13), \\ \log(\sigma_i \text{ ratio}) &= (0.57 \pm 0.15)\log T + (0.21 \pm 0.10), \end{aligned}$$

where T is the ratio of observed timespan after to before, and \pm refers to 95% confidence intervals. Considering separately the objects observed in the days to weeks after discovery, the σ_a , σ_e and σ_i regression slopes were all close to 1.0. For the objects recovered at a new opposition, the slope was 1.0 for σ_a , and 0.6 for σ_e and σ_i (but 1.0 marginally permitted at 95% confidence for both). A value of 1.0 would imply that the proportional orbital improvement equals the proportional increase in observed timespan. In practice, the number and distribution of observations

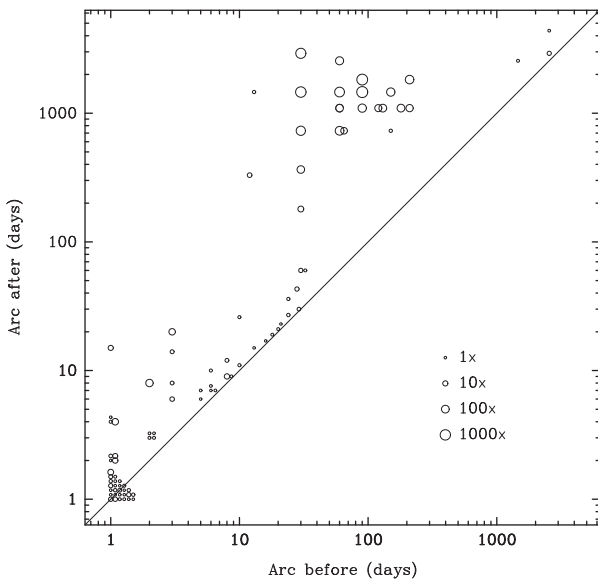


Fig. 3. Orbital improvement as a function of observational timespan. Distance above diagonal line corresponds to factor by which observed arc has increased. Size of each circle shows factor by which uncertainty in a has improved as a result of increase in observed arc. Points near (1 day, 1 day) have been slightly separated for clarity.

within the timespan, and the accuracy of the observations, also affect the orbital quality (cf. Muinonen et al., 1994).

Based on the analyzed datasets, we conclude that the most important orbital contribution is the rapid follow-up of newly discovered NEAs (few days to one month after discovery). Another contribution is the recovery of NEAs at a new opposition which enlarges orbital arcs by a few months or years. Obviously, VIs and PHAs have priority over regular NEAs. Most important are fainter objects ($V > 21$) which could remain invisible to the available 1–2 m surveys and could result in insecure orbits or lost objects not being observed for the next few years.

3.2. Known MBAs

Many known MBAs were serendipitously encountered, identified, measured and reported in the large field images taken by Blanco MOSAIC II and INT WFC cameras. In total, 1699 positions corresponding to 288 known MBAs were reported during our Blanco Mosaic II run, while 3465 positions of 580 known MBAs were reported from the observed INT-WFC fields.

In Fig. 4 we plot the O–C astrometric residuals corresponding to our reported positions of the known MBAs encountered in all Blanco and INT fields. The first panel plots the residuals for the Blanco run clearly affected by the field distortion of the MOSAIC II camera, with a root mean square of the O–C residuals 0.90'' and some values larger than 2'' for the objects measured far from the center of the camera. In the second panel we plot the residuals for the INT-WFC fields observed during December 2011 and February 2012 runs (3465 positions). All the INT-WFC images were reduced with THELI software (Erben et al., 2005) which corrected the field distortion across the whole WFC field. The INT (right) O–C plot in Fig. 4 shows the accuracy of the WFC astrometry improved after field correction (RMS of O–C residuals 0.41''). By comparison, a similar INT-WFC plot in our previous paper (Fig. 4b from Vaduvescu et al., 2011) includes WFC data processed without THELI and shows an RMS more than double around the origin (0.97'').

Some inhomogeneity could be observed comparing the INT NEA O–C plot (Fig. 2) with the INT MBA plot (Fig. 4), namely the NEA plot seems more elongated towards the α direction while the MBA plot is more symmetric in both α and δ . This is explained by the fact that residuals for NEAs are larger than for MBAs due to the measurement errors caused by NEAs moving faster in α than in δ .

3.3. Unknown objects

Working in a team, we could detect visually and measure all moving objects appearing in all fields observed with the INT and Blanco telescopes. All CCD images were bias corrected and flat fielded using IRAF or other image processing software, and only the WFC images were corrected for field distortion with THELI software (Erben et al., 2005). We used Astrometrica (Raab, 2012) to identify all moving sources in the WFC and MOSAIC II paired CCDs based on the MPCORB asteroid database retrieved soon after the observing date. We measured and reported all the unknown objects which were later characterized by determining preliminary orbits using the FIND_ORB software (Gray, 2012) in batch mode. Their main orbital parameters (a , e , i and MOID) are given in the Appendix Tables A3–A7. Based on the observed fields and runs, we distinguish the following lists which total 1090 previously unknown asteroids:

- 104 unknown objects discovered mostly during multiple nights in the February 2012 WFC opposition fields (Table A3);

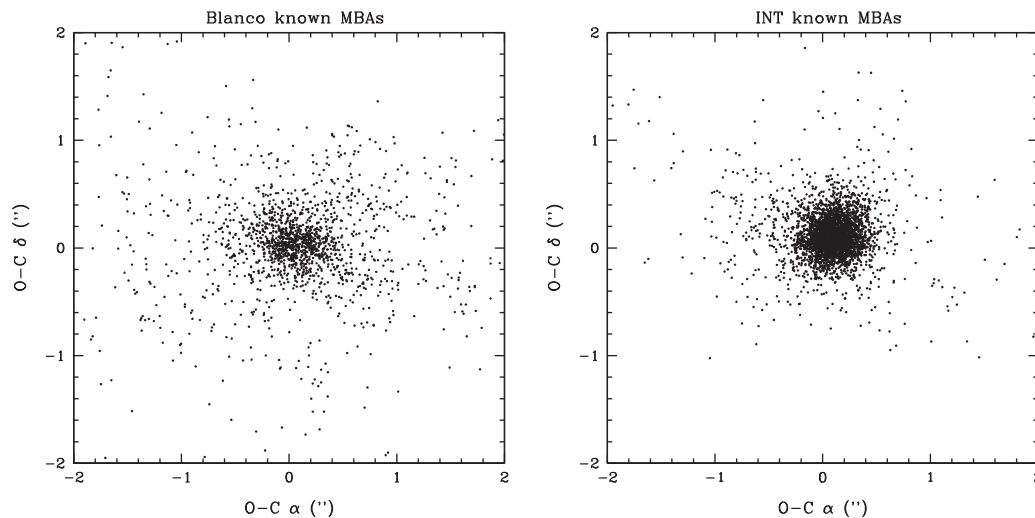


Fig. 4. O–C (observed minus calculated) residuals for known MBAs observed with Blanco and INT. INT-WFC images were corrected with THELI for field distortion, decreasing residuals across the whole field to RMS standard deviation 0.41".

- 626 unknown objects observed with the INT during one night in February 2012 in the opposition mini-survey fields (Table A4);
- 89 unknown objects observed with the INT in February 2012 in program NEA fields (Table A5);
- 75 unknown objects observed with the INT during 2011 runs in program NEA fields (Table A6);
- 196 unknown objects observed with Blanco telescope during one night in 2011 in program NEA fields (Table A7).

3.3.1. Discovered MBAs

104 unknown objects could be recovered during multiple nights in the February 2012 WFC opposition mini-survey, thus they have been given provisional designations and should soon become credited MBA discoveries of our EURONEAR program using the INT WFC. For these 104 discovered objects, Appendix Table A3 lists firstly their orbital elements a , e , i and MOID (calculated with FIND_ORB in batch mode) based on observational data from our run only (linked by the MPC), and secondly their published MPC orbits based on all available observations in the MPC database (accessed 8 August 2012). The calculated FIND_ORB orbits are similar to those published by the MPC for the majority of our discovered MBAs, with standard deviations 0.26 AU in a , 0.14 in e , 3.78 deg in i and 0.30 AU in MOID. In fact the MPC orbits are calculated mostly using our data alone, but in some cases eventually adding other observations from elsewhere before or following our runs.

3.3.2. Unknown MBAs

The great majority of the 1090 unknown objects detected in the INT and Blanco runs could be characterised as MBAs, their proper motion and preliminary orbits matching the known main belt population well. We include the remaining unknown objects in Appendix Tables A4–A7, listing orbital elements a , e and i obtained by FIND_ORB automated fitting of our observational data. Due to the very short arcs derived from one night observations, the FIND_ORB preliminary orbits should be regarded with caution. Nevertheless, FIND_ORB was found to fit most orbits quite accurately, following direct comparison of one night fitted orbits with published orbits based on all available observations, and also after comparison with the whole known asteroid population via the classic a – e and a – i plots (Figure 7 of Vaduvescu et al., 2011) which can be virtually reproduced using the 1090 preliminary orbits found here.

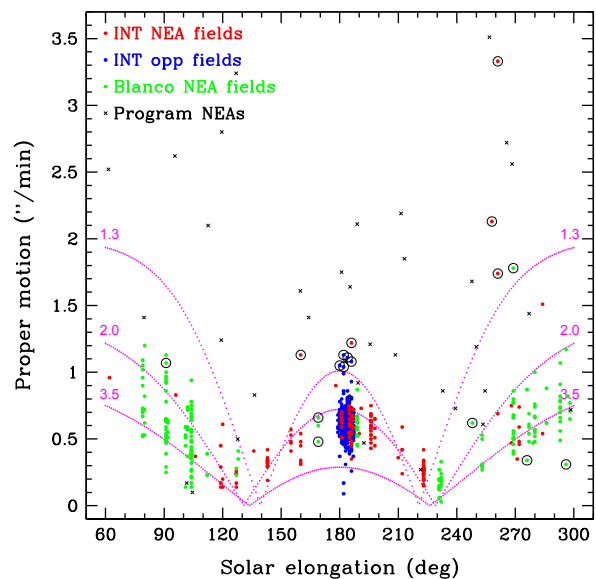


Fig. 5. Using the ϵ – μ orbital model (Vaduvescu et al., 2011) to check NEO candidates based on direct observational quantities solar elongation (ϵ) and proper motion (μ). We plot with solid symbols all unknown objects observed with Blanco (green) and the INT (red for objects observed in program NEA fields and blue for objects observed in opposition fields). The three overlaid dotted magenta curves correspond to asteroids orbiting between $a=2.0$ and $a=3.5$ AU (main belt) and $a=1.3$ AU (NEO limit). We mark with circles the 18 best NEO candidates labeled in bold in the Appendix Table A8. The fast NEO candidate ESU031 (identified with the known NEA 2012 DC28) is located above the plot, matching the model. With black crosses we plot the 47 program NEAs (which include 11 fast objects located above the plot), most of them (38 objects or 81%) matching the ϵ – μ model. (For interpretation of the references to color in this figure caption, the reader is referred to the web version of this article.)

3.3.3. NEO candidates

Following our previous work which analyzed data taken with 1–2 m telescopes (Vaduvescu et al., 2011), we use three independent search methods to check the unknown objects for Near Earth Objects (NEOs) observed with 2–4 m facilities. The first method employs our model presented by Vaduvescu et al. (2011) which plots the two directly observed quantities μ (apparent proper motion) and ϵ (solar elongation, ϵ above 180 deg corresponding to sky directions east of opposition). Using this model (Fig. 5), one can distinguish NEO candidates (located above the $a=1.3$ AU

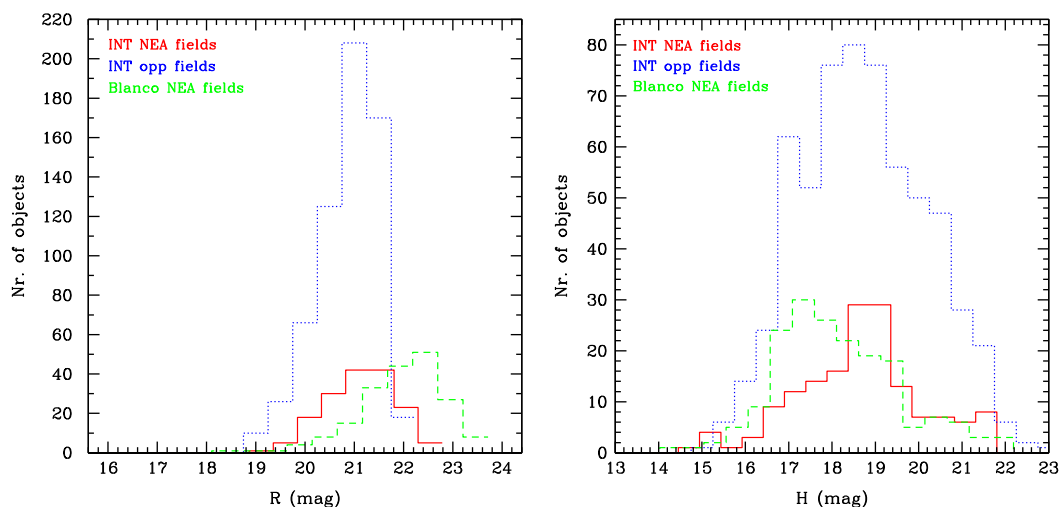


Fig. 6. Number of unknown objects as a function of observed apparent R magnitude and calculated absolute magnitude H for the INT dataset (red solid line for NEA fields, blue dotted line for opposition fields) and Blanco (green dashed line for NEA fields). (For interpretation of the references to color in this figure caption, the reader is referred to the web version of this article.)

dotted magenta curve corresponding to the NEO limit) from MBA objects (located below the $a=2.0$ AU curve). The last column of Appendix Table A8 lists the result of this fit as “Best”, “Good”, “Close” or “Bad” with respect to this model, considering only objects flagged “Good” or “Best” as NEO candidates.

Our second NEO search method uses the “NEO Rating” server developed by the MPC (2012b) which calculates a score for NEO candidates based on their expected proper motion compared to the MBA distribution. In the second last column of Table A8 we include the MPC rating on a scale from 0% (worst) to 100% (best fit), considering objects having scores higher than 10% as NEO candidates.

Our third NEO search method uses the MOIDs of the preliminary orbits calculated with FIND_ORB. It should be regarded with caution because of the small observed arcs, but can indicate possible NEOs. We take $\text{MOID} < 0.3$ AU as the criterion for NEO candidates (Table A8).

From 1090 unknown objects observed with INT and Blanco (Tables A3–A7), we find 60 NEO candidates defined as satisfying at least one of the three search methods (Table A8). To allow a safer selection, we highlight 18 *best NEO candidates* defined as unknown objects matching at least two of the three selection methods (bold in Table A8 and marked with circles in Fig. 5).

Five of these 18 best NEO candidates were observed with the INT in 2012 and 2011 in program NEA fields: EBA012, EPA015, VFLLP01, VKF008 and VKF034. The first three fulfilled all three NEO search criteria. EBA012 was quite a fast moving object ($\mu = 2.13''/\text{min}$) observed in the field of NEA 2012 BB14 (recovered and published). EPA015 was a fairly bright object ($R=19.6$) observed in the field of the NEA 2011 FR29 (recovered and published). It too was among the fastest of the best NEO candidates ($\mu = 3.33''/\text{min}$), which classifies it as a NEA. VFLLP01 was a relatively faint object ($R=21.7$), encountered at 12 September 2011 as the only object in the field of PHA 2011 BN24 (not found at $V=21.6$), although the EURONEAR O–C calculator does not show any correlation between the two objects. Its FIND_ORB fit is very unstable based on the least squares, Herget or downhill simplex methods, thus its calculated orbit should be regarded with caution.

Six best NEO candidates were observed with the INT during 2012 in the opposition mini-survey: EBA023, EPA143, EPA190, EPO031, EPO065 and ESU031 (Table A8). ESU031 represents our fastest NEO candidate at $\mu = 10.32''/\text{min}$, producing long trails in three 180 s exposures taken in the opposition OP5 mini-survey

field observed during the first night 25 February 2012. We promptly reduced and submitted three positions to MPC, but the robot matched it with 2012 DC28, an NEA discovered only two days before by the Catalina survey. EPO031 fulfils all three NEO selection criteria and has relatively high brightness ($R=19.6$): the MPC linked it with an object seen by Catalina, designating it 2012 DL54, but its orbit is still indeterminate.

The remaining seven best NEO candidates were observed with the Blanco telescope: PCTV024, PCTV026, PCTVb50, PCV023, PCVP005, PCVP007 and PCVS024 (Table A8). The first two were encountered in the field of PHA 2008 YS27 (not found). PCTV024 is the brightest ($R=18.3$) of our 18 best NEO candidates, with MPC score 100% and estimated MOID close to the NEA limit (0.28 AU). PCTV026 is a very similar object measured only in three images. However, both objects give a $e-\mu$ “Bad” flag, while their measured magnitudes are highly uncertain (despite their brightness), being affected by the very high Milky Way star density seen with the 4 m telescope. PCV023 is a relatively fast object $\mu = 1.78''/\text{min}$ and, as the only one of the seven Blanco objects meeting all three NEO search criteria, is among the most promising of all our best NEO candidates.

4. Discussion

4.1. Comparison between NEO search methods

At present (October 2012) 16 of the 18 best NEO candidates (Section 3.3.3) remain as one-night objects, with one (2012 DC28) confirmed as a certain NEA. We test the suitability of the three NEO search criteria by applying them to objects known to be NEOs, namely the 47 program NEAs observed with INT and Blanco. We test the search methods using our observed small arcs only (knowing the objects to be NEOs from the MPC published orbits based on all available observations).

To test the $e-\mu$ model, in Fig. 5 we plot with crosses all 47 program NEAs. About 38 objects (81%) are confined above the NEO limit, while nine outliers have very elliptical orbits, namely 2008 QT3 ($e=0.52$), 2011 AG5 ($e=0.39$) and 2010 XC25 ($e=0.53$) at bottom-left of the plot, 2011 XZ1 ($e=0.46$) and 2009 OG ($e=0.86$) close to opposition, and 2008 XB1 ($e=0.37$), (175 706) ($e=0.35$), (175 189) ($e=0.39$) and 2007 JF22 ($e=0.59$) at bottom-right of the plot.

Using the same 47 program NEA sets of observations, the NEO rating tool has 36 of them (77%) satisfying the recommended MPC $Int > 50\%$ limit (MPC, 2012b). Of the remaining 11 objects, 8 also fail the $\epsilon-\mu$ model, namely: 2008 QT3 (Int score 15%), 2010 XC25 (25%), 2011 XZ1 (3%), 2009 OG (17%), 2008 XB1 (20%), (175 706) (score 23%), (175 189) (27%) and 2007 JF22 (score 4%). Three other outliers are 2009 EE81 (10%), 2006 CT10 (16%) and 2012 AC13 (rate 47%). Only two objects have a NEO score below 10%, supporting this limit as a safe threshold for our selection method of NEO candidates.

Running FIND_ORB for the same 47 program NEAs, using only our short observed arcs, MOIDs of 11 objects result larger than the NEO limit of 0.3 AU, i.e. 36 (76%) would be NEOs according to this test. Nevertheless, comparing these estimated MOIDs to the more accurately known MOIDs from MPC published orbits based on all available observations, the standard deviations are quite large, namely 0.90 AU in a , 0.34 in e , 12.9 deg in i and 0.28 AU in the MOID, thus the values of the FIND_ORB fitted orbits of NEAs based on very small arcs should be regarded with great caution.

In comparison the same three search criteria applied to our unknown objects resulted in 13 objects as NEO candidates according to the $\epsilon-\mu$ model (flags “Best” or “Good”), 26 objects according to the MPC “NEO rating” selection (Int score $> 10\%$), and 41 objects according to their FIND_ORB fitted orbits (MOID < 0.3 AU), with 18 best NEO candidates satisfying at least two of these criteria (Section 3.3.3). Based on this data sample, the $\epsilon-\mu$ model closely followed by the NEO Rating appears to be the safest method to flag one-night NEO candidates.

4.2. Comparison between 2 m and 4 m facilities

The Blanco 4 m run consisted of only one dark clear night, partially affected by thin clouds. The INT runs consisted of about four mostly dark clear nights in all, three during the February 2012 run, and time totalling about one night during four nights in 2011. Thus, the INT 2.5 m data could be more representative statistically than the Blanco 4 m data.

In Fig. 6 we plot histograms counting the unknown objects as a function of the observed R magnitude (left) and calculated absolute magnitude H (right) based on the three available datasets: the INT NEA fields (2011 and 2012), INT opposition fields (2012), and Blanco NEA fields. According to the left plot, the Blanco telescope sampled about 2 mag deeper than the INT, being most efficient in detection around $R \sim 22.5$ and reaching a limit of $R \sim 24$. The INT was most efficient around $R \sim 21$ and reached a limit $R \sim 22$. Based on the left tail of the total distribution, apparently there are no more unknown objects brighter than $R \sim 19$ to discover nowadays. The INT limit is higher by about 0.8 mag than our past results ($R \sim 21.2$ in Vaduvescu et al., 2011), probably due to better weather conditions in 2011–2012. Also, the INT limit appears to surpass by about 0.5 mag our past dark time ESO/WFI limit ($R \sim 21.5$). The H histogram suggests that the Blanco telescope is finding a higher proportion of larger (brighter H) objects than the INT, presumably because many of these unknown objects are at larger distances (thus fainter R), i.e. Blanco tends to see further out into the main belt.

Table 2 summarizes data derived from Blanco and INT runs, in observed NEA fields and opposition (opp.) fields. Based on the O–C residuals, the astrometric quality for program NEAs observed mostly in the center of the fields is identical for the two cameras, with a root mean square of the O–C residuals of $0.46''$. Nevertheless, the astrometry of the known MBAs recovered across the whole MOSAIC II field is more than two times worse (RMS $0.97''$) due to the uncorrected field of Blanco at its prime focus, compared with the INT WFC (RMS $0.41''$).

Table 2

Summary and statistics based on the Blanco and INT runs.

Observations	Blanco	INT	Total
Recovered NEAs	14	33	47
Nr. of positions	94	221	315
O–C standard deviation (")			
... program NEAs	0.46	0.46	–
... known MBAs	0.97	0.41	–
Known MBAs	288	580	868
... in NEA fields	288	132	420
... in opp. fields	–	448	448
Nr. of positions	1699	3465	5164
Unknown objects	196	790	986
... in NEA fields	196	164	360
... in opp. fields	–	626	626
Nr. of positions	1301	4025	5326
Discovered objects	–	104	104
Nr. of positions	–	1153	1153
Nr. of observing nights	1	4	5
Nr. of program NEA fields	28	47	75
Nr. of opp. fields	–	40	40
Total nr. of fields	28	87	115
Total nr. of CCD images	224	348	572
Sky coverage (sq. deg)	10	24	34
... NEA fields (sq. deg)	10	13	23
... opp. fields (sq. deg)	–	11	11
Limiting magnitude (R)	24.0	22.0	–
Apparent magnitude peak (R)	22.5	21.0	–
Total nr. of objects	498	1507	2005
Total nr. of positions	3094	8864	11,958
Known MBA density (obj/sq. deg)			
... in NEA fields	29	10	–
... in opp. fields	–	41	–
Unknown MBA density (obj/sq. deg)			
... in NEA fields	19	13	–
... in opp. fields	–	66	–
Unknown NEO density (obj/sq. deg)	0.7	0.5	–

Counting the unknown and known asteroids (mostly MBAs) encountered in the Blanco and INT fields, we could assess the ratio of the density of unknown to known MBAs in any 4 m and 2 m class survey. The 87 observed WFC fields give this ratio for the INT as 1.6 in opposition fields and 1.2 in program NEA fields, thus an average of 1.4. This fraction is very consistent with the 1.3 result based on ESO/MPG data from our previous work and is higher than our past 0.8 result based on previous INT data affected by bad weather (Vaduvescu et al., 2011). Counting the unknown and known objects observed with Blanco during one night in 28 fields, the ratio is 0.7 for Blanco, unexpectedly smaller than that from the INT. This inconsistency could be explained due to poor statistics affected by weather and field selection. During the first part of the only Blanco night the clouds and cirrus strongly affected 9 fields from the total of 28 observed. Four other fields were in the Milky Way and could not be scanned for objects (other than the program NEAs) due to the extreme star density there. Also, seven other fields were observed at high ecliptic latitude and could not serve for statistics. Eliminating all these fields, we selected five fields with limiting detection magnitude $R \sim 23$ (2008 XB1, 2008 DJ, 2008 EP6, 2010 XC25 and 2009 CS), more suitable for statistics. Based on this selection, we derive the ratio 2.7 for Blanco in relatively good weather conditions. In conclusion, Blanco could discover about twice as many unknown MBAs with respect to known MBAs (ratio 2.7) compared with the INT (ratio 1.4),

assuming similar good weather and dark sky conditions for both facilities.

4.3. Statistics of the unknown MBA and NEO population

Next we derive some statistics based on the data obtained from 10 square degrees covered by Blanco and 24 square degrees covered by the INT (11 square degrees near opposition and 13 square degrees in random NEA fields).

4.3.1. Unknown MBA density

An average of 29 known MBAs and 20 unknown MBAs per square degree could be observed with Blanco based on our small analyzed sample (mostly far from ecliptic) partially affected by poor weather. The best two fields observed in good conditions in the ecliptic (2010 XC25 and 2009 CS, both far from opposition) give similar densities to each other and an average of 45 known MBAs and 90 unknown MBAs per square degree, thus a total of 135 MBAs per square degree visible with the Blanco 4 m telescope (two unknown to every one unknown asteroid) up to $R \sim 23$. This density based on small non-opposition statistics is comparable with the work of Yoshida and et al. (2003) who counted 208 MBAs per square degree up to $R \sim 23.0$ based on the opposition SMBAS-I survey and 182 MBAs per square degree to the same limit from the SMBAS-II survey (Yoshida and Nakamura, 2007).

Based on our larger INT dataset, 41 known and 66 unknown MBAs per square degree could be detected in average in the observed fields. Thus, a total of 107 MBAs per square degree (1.6 unknown to every 1 known objects) could be detected at opposition by the INT up to $R \sim 22.0$. This density is comparable with our previous result of 63 MBAs per square degree (27 known, 36 unknown) based on a similar survey using ESO/MPG (Vaduvescu et al., 2011) up to a limit 0.5 mag shallower. The SMBAS surveys when counted to the same $R = 22.0$ limit give 128 objects per square degree (Yoshida and et al., 2003) and 103 objects per square degree (Yoshida and Nakamura, 2007), very close to our present INT result.

4.3.2. Unknown NEA density

Considering the best NEO candidates marked in bold in the Appendix Table A8, we estimate the unknown NEO density detectable in 2 m and 4 m surveys. Counting six NEO candidates in the INT NEA fields covering 13 square degrees, we derive an average of 0.5 NEOs per square degree observable with the INT. This is in very good agreement with five best NEO candidates observed in the INT opposition fields covering 11 square degrees and also within the range of our previous results (between 0.2 and 0.6 objects per square degree based on the ESO/MPG and from 0.1 to 0.8 for the INT, Vaduvescu et al., 2011). In the Blanco program NEA fields covering 10 square degrees, we count seven best NEO candidates, thus 0.7 NEOs per square degree observable with the Blanco telescope; this number should be regarded as a minimum, based on poor weather during the only available Blanco night.

The MPC lists 609,956 known asteroids and 9242 known NEAs in its database (checked 25 October 2012), a ratio of 1 in 66. Our NEO candidate list (Table A8) comprises 60 NEO candidates from which only 18 are the best NEO candidates. Taking into account our total of 1090 unknown objects observed with Blanco and INT, we derive a ratio of one NEO candidate for every 18 asteroids and one best NEO candidate for every 60 unknown asteroids. This ratio comes very close to the above known MPC ratio of 66, validating our NEO candidate selection method.

4.3.3. Total number of NEAs observable by a 2 m survey

Based on the 11 best NEO candidates discovered in 24 square degrees surveyed with the INT, we can evaluate the total number of unknown NEOs detectable by a 2 m-class telescope. Checking the orbital distribution of our NEO candidates (11 INT objects in bold in the Appendix Table A8) we observe that all these objects have inclination $i < 25^\circ$ (although the uncertainties are expected to be large due to small observed arcs). Considering the whole known NEA population (NEODyS 2012), we derive 86% NEAs having $i < 25^\circ$, so we adopt the same percentage for our statistical analysis. The area of the celestial sphere between ecliptic latitudes -25° and $+25^\circ$ represents 17400 square degrees, namely about 42% from the total area of a sphere. Extrapolating our number of 11 objects observed in 24 square degrees within the ecliptic zone $-25^\circ < \beta < +25^\circ$, we derive about 8000 unknown best NEO candidates having $i < 25^\circ$. Extrapolating in turn this number to all inclinations, we conclude that there are in total some 9300 unknown NEO candidates observable with a 2 m survey. Adding this number to the currently known almost 10000 NEAs (discovered by 1–2 m surveys), we predict about 19300 NEAs observable by 2 m surveys. This number is very close to Mainzer and et al. (2012) who used NEOWISE data to predict a total of $20,500 \pm 4200$ NEAs larger than 100 m, which could be regarded as a limit for 2 m surveys.

5. Conclusions and future work

In this paper we report on the follow-up and recovery of 477 program NEAs, PHAs and VIs observed mostly between 2010 and 2012 from nine sites of the EURONEAR network which include six professional 1–4 m class telescopes located in Chile, La Palma, France and Germany plus three smaller educational and public outreach telescopes in Romania and Germany. The addition of these objects to our previous work leads to a total of 739 NEAs followed-up by the EURONEAR network since 2006.

The reduced data presented in this paper generated 98 MPC publications. We use the most important data to study the orbit improvement of 111 NEAs, PHAs and VIs, among which 29 objects were recovered at a new opposition and the other 82 were followed-up soon after discovery. Although recovery of NEAs a few years after their last observation appears to be important, follow-up of newly discovered objects soon after discovery seems to be more valuable for the recovery and orbital improvement of fainter and highly uncertain objects which could remain invisible to existing surveys.

We characterize each site based on the astrometric residual plot for all observed NEAs, finding WHT-ACAM, INT-WFC and Blanco-MOSAIC II (close to center only) the best instruments (RMS of the O–C 0.44–0.46"), followed by Bonn and Galati (0.56–0.57"), particularly good small educational facilities. Using our published data of known MBAs, we compare the astrometry across the large field of the INT-WFC and Blanco-MOSAIC II and also the astrometric improvement over the whole field of the INT-WFC after image correction of its quite distorted prime focus field, reaching RMS 0.41", more than two times better than 0.97", our past results without THELI correction.

During two runs plus a few other discretionary hours (equivalent to five clear nights in total) we used the large field INT-WFC and Blanco-MOSAIC II facilities to recover and follow-up 47 highly uncertain NEAs and also to carry out an opposition mini-survey with the INT (10 square degrees) focused on MBAs. In 115 fields observed with these two 2–4 m large field facilities covering a total of 34 sky square degrees we carefully measured and reported to the MPC, in addition to the 47 program NEAs, all identified moving objects, comprising 868 known MBAs, 986 unknown

objects—mostly MBAs, and 104 newly discovered MBAs. We use these data to derive new MBA and NEA observability statistics for 2–4 m surveys, continuing our previous work based on data obtained using 1–2 m large field facilities. The INT or any similar 2 m-class telescope can observe NEAs as faint as $R \sim 22$, being most efficient in discovery of MBAs around $R \sim 21$, while Blanco or a similar 4 m class facility can detect NEAs up to $R \sim 24$, being most efficient to discover new objects around $R \sim 22.5$. Based on our INT dataset, a total of 107 MBAs per square degree can be detected at opposition up to $R \sim 22.0$ in a 2 m survey (this density surpassing our 2 m past results but remaining very close to other results based on surveys using larger telescopes). The two best fields observed with Blanco in the ecliptic in good weather conditions result in 135 MBAs per square degree to $R \sim 23$.

The ratio of unknown to known MBAs observable by a 2 m or 4 m class survey is 1.4 based on our INT data (very consistent with our past work) and 2.7 based on a few fields observed in good weather with Blanco, which could discover twice as many unknown MBAs with respect to known MBAs than the INT.

About 104 new MBAs were recovered in two or three nights during our opposition mini-survey using the INT, so we expect them to be credited in the future as EURONEAR MBA discoveries. We studied our 986 one-night unknown objects observed with Blanco and the INT using three independent NEO search criteria, finding 60 NEO candidates satisfying at least one criterion and 18 best NEO candidates satisfying at least two. Using our total sky coverage (24 square degrees with INT and 10 square degrees with Blanco) and counting the best NEO candidates, we derived an average of 0.5 NEO candidates per square degree observable in a 2 m survey (in very good agreement with our past results) and at least 0.7 NEO candidates per square degree based on our one Blanco night partially affected by clouds. The ratio of unknown objects over best NEO candidates observed with INT and Blanco is 60, in very good agreement with the ratio of 66 obtained when using the entire known published asteroid and NEA populations. *Using the 11 best NEO candidates observed with the INT in 24 square degrees and a simple two step orbital model, we assess the total number of NEAs detectable by a 2 m survey to 19300 objects, in very close agreement with a recent work.*

We conclude by listing two future projects aiming to continue the study of the NEA distribution at the faint end, using data from existing large field 4–8 m class telescopes. The first facility is the new DECam camera installed on the Blanco telescope. Second is the SuprimeCam camera on Subaru (based on archival data related to another EURONEAR data-mining project) and also the new Subaru Hyper-SuprimeCam camera, which could yield extensive statistics allowing existing NEO models to be checked and the formation and evolution of the entire NEA population to be studied. These facilities could be scanned using automated detection software, then comparing results with human search based on our experience and other independent studies.

Acknowledgments

Special thanks are due to the science committees and institutions awarding time to our EURONEAR proposals: the Chilean National Time Committee (for the Blanco observing run 0646, 3–4 June 2011) and the Spanish Time Allocation Committee (for the INT observing run C6, 25–28 February 2012). Special thanks are due to the Isaac Newton Group (ING), the U.K. Science and Technology Facilities Council (STFC), the Spanish “Ministerio de Ciencia e Innovación” (MICINN) and the “Instituto Astrofísico de Canarias” (IAC) for supporting the project AYA2008-06202-C03-02 thanks to six visiting students who received funding for their INT observing run. M. Karami thanks the Iranian National Observatory

project for the INT training opportunity and the INT observing nights. To correct the optical field distortions of the INT-WFC images we used THELI software; thanks are due to M. Schirmer for his assistance in using it. Acknowledgments are due to Bill Gray for providing, developing and allowing free usage of FIND_ORB to the entire amateur-professional community. We thank the Minor Planet Center, especially T. Spahr and G. Williams who revised our MPC reports. Thanks are also due to the two referees who provided feedback important to improve our paper. This research has made intensive use of the Astrometrica software developed by Herbert Raab, very simple to install and use by students and amateur astronomers. We also used the image viewer SAOImage DS9, developed by Smithsonian Astrophysical Observatory and also IRAF, distributed by the National Optical Astronomy Observatories, operated by the Association of Universities for Research in Astronomy, Inc. under cooperative agreement with the National Science Foundation.

Appendix A. Supplementary data

Supplementary data associated with this article can be found in the online version at <http://dx.doi.org/10.1016/j.pss.2013.06.026>.

References

- Apitzsch, R., et al., 2011. MPEC 2011-E19.
- Arlot, J.E., et al., 2010a. MPC 69732, 12.
- Arlot, J.E., et al., 2010b. MPC 72456, 4.
- Bacci, P., et al., 2012. MPEC 2012-B17.
- Balam, D.D., et al., 2011. MPC 75940, 4.
- Birlan, M., et al., 2010a. *Astronomy & Astrophysics* 511, 40.
- Birlan, M., et al., 2010b. MPC 70198, 9.
- Birlan, M., et al., 2010c. MPEC 2010-W11.
- Birlan, M., et al., 2010d. MPEC 2010-W12.
- Birlan, M., et al., 2010e. MPEC 2010-W13.
- Birlan, M., et al., 2011a. MPEC 2011-E11.
- Birlan, M., et al., 2011b. MPEC 2011-E12.
- Birlan, M., et al., 2011c. MPEC 2011-E13.
- Birlan, M., et al., 2011d. MPEC 2011-W29.
- Birlan, M., et al., 2011e. MPEC 2011-W33.
- Borngen, F., Stecklum, B., 2012a. MPC 79140, 1.
- Borngen, F., Stecklum, B., 2012b. MPC 79473, 5.
- Bottke, W.F., et al., 2006. *The Annual Review of Earth and Planetary Sciences* 34, 157.
- Bowell, E., Muinonen, K., 1994. Earth-crossing asteroids and comets: groundbased search strategies. In: Gehrels, S. (Ed.), *Hazards Due to Comets and Asteroids*. University Arizona Press, p. 149.
- Bressi, T.H., et al., 2012. MPEC 2012-D102.
- Buie, M.W., et al., 2011a. MPC 74496, 6.
- Buie, M.W., et al., 2011b. MPC 75198, 5.
- Buie, M.W., et al., 2011c. MPC 75623, 6.
- Buie, M.W., et al., 2011d. MPC 75939, 2.
- Buie, M.W., et al., 2011e. MPC 76865, 5.
- Buie, M.W., et al., 2012. MPC 79528, 6.
- Buzzi, L., et al., 2011a. MPEC 2011-W12.
- Buzzi, L., et al., 2011b. MPEC 2011-W22.
- Buzzi, L., et al., 2011c. MPEC 2011-W27.
- Buzzi, L., et al., 2011d. MPEC 2011-W28.
- Buzzi, L., et al., 2011e. MPEC 2011-W44.
- Buzzi, L., et al., 2011f. MPEC 2011-W45.
- Buzzi, L., et al., 2011g. MPEC 2011-W52.
- Cavadore, C., et al., 2011a. MPC 74036, 3.
- Cavadore, C., et al., 2011b. MPC 77173, 6.
- Christensen, E.J., et al., 2012. MPEC 2012-J34.
- Eglitis, I., et al., 2012. MPEC 2012-H42.
- Elst, E.W., et al., 2011a. MPC 76441, 4.
- Elst, E.W., et al., 2011b. MPC 77265, 3.
- Erben, T., et al., 2005. *Astronomische Nachrichten* 326, 432. (THELI software).
- EURONEAR, 2012a. The European Near Earth Asteroids Research (<http://euronear.imcce.fr>).
- EURONEAR, 2012b. Observing Tools: Planning (<http://euronear.imcce.fr/tiki-index.php?page=Planning>).
- Farinella, P., et al., 1993. *Icarus* 101, 174.
- Fitzsimmons, A., et al., 2011a. MPC 76443, 2.
- Fitzsimmons, A., et al., 2011b. MPC 74148, 2.
- Fitzsimmons, A., et al., 2011c. MPC 74893, 1.

- Fitzsimmons, A., et al., 2011d. MPC 75207, 2.
 Fitzsimmons, A., et al., 2011e. MPC 77266, 1.
 Fitzsimmons, A., et al., 2012a. MPC 78047, 5.
 Fitzsimmons, A., et al., 2012b. MPC 78437, 11.
 Fitzsimmons, A., et al., 2012c. MPC 78894, 9.
 Fitzsimmons, A., et al., 2012d. MPC 79221, 1.
 Fitzsimmons, A., et al., 2012e. MPC 79530, 1.
 Gajdos, S., et al., 2012. MPEC 2012-E19.
 Gray, B., 2012. FIND_ORB (http://www.projectpluto.com/find_orb.htm).
 Holman, M., et al., 2011. MPC 75625, 2.
 Jaeger, M., et al., 2012. MPEC 2012-H90.
 Lang, D., et al., 2010. *Astronomical Journal* 139, 1782L.
 Lehmann, G., et al., 2011. MPEC 2011-E14.
 Mainzer, A., et al., 2012. *The Astrophysical Journal* 752, 110.
 McMillan, R., et al., 2011. MPEC 2011-W25.
 Milani, A., Gronchi, G.F., 2009. Theory of Orbit Determination.
 Morbidelli, A., et al., 2002. Origin and evolution of near-earth objects. In: Bottke, et al. (Eds.), *Asteroids III*. University Arizona Press, p. 409.
 Minor Planet Center (MPC), 2012a. (<http://www.minorplanetcenter.net>).
 MPC, 2012b. NEO Rating (<http://www.minorplanetcenter.net/iau/NEO/PossNEO.html>).
 Muinonen, K., Bowell, E., Wasserman, L.H., 1994. *Planetary and Space Science* 42 (4), 307.
 NASA JPL, 2012. Sentry Risk Table (<http://neo.jpl.nasa.gov/risk>).
 Nishiyama, K., et al., 2011. MPEC 2012-J01.
 Near Earth Objects—Dynamic Site (NEODyS), 2012 (<http://newton.dm.unipi.it/neodyS>).
 Raab, H., 2012. Astrometrica Software (<http://www.astrometrica.at>).
 Sonka, A., 2008. MPC 64104, 11.
 Sonka, A., 2009a. MPC 65048, 3.
 Sonka, A., 2009b. MPC 65638, 6.
 Sonka, A., 2009c. MPC 65928, 13.
 Sonka, A., 2009d. MPC 67139, 5.
 Sonka, A., 2009e. MPC 67404, 7.
 Sonka, A., 2009f. MPC 67677, 8.
 Sonka, A., 2010a. MPC 69817, 4.
 Sonka, A., 2010b. MPC 71094, 4.
 Sonka, A., 2010c. MPC 72053, 3.
 Sonka, A., 2011a. MPC 75208, 6.
 Sonka, A., 2011b. MPC 75447, 3.
 Sonka, A., 2011c. MPC 77270, 7.
 Sonka, A., 2012a. MPC 77702, 7.
 Sonka, A., 2012b. MPC 78050, 8.
 Sonka, A., 2012c. MPC 79998, 13.
 Spaceguard System, 2012. Priority List (<http://spaceguard.iaps.inaf.it/SSystem/SSystem.html>).
 Stecklum, B., 2012a. MPC 79746, 2.
 Stecklum, B., 2012b. MPC 79971, 5.
 Stecklum, B., et al., 2012a. MPEC 2012-K07.
 Stecklum, B., et al., 2012b. MPEC 2012-G45.
 Tercu, O., Dumitriu, A., 2011a. MPC 75947, 2.
 Tercu, O., Dumitriu, A., 2011b. MPC 76451, 8.
 Tercu, O., Dumitriu, A., 2011c. MPC 76874, 7.
 Tercu, O., Dumitriu, A., 2011d. MPC 77273, 6.
 Tercu, O., Dumitriu, A., 2012a. MPC 77705, 1.
 Tercu, O., Dumitriu, A., 2012b. MPC 78053, 2.
 Tercu, O., Dumitriu, A., 2012c. MPC 78445, 7.
 Tercu, O., Dumitriu, A., 2012d. MPC 78902, 10.
 Tercu, O., Dumitriu, A., 2012e. MPC 79225, 1.
 Tercu, O., Dumitriu, A., 2012f. MPC 79533, 5.
 Tercu, O., Dumitriu, A., 2012g. MPC 80000, 11.
 Tudorica, A., 2011. MPC 74509, 1.
 Tudorica, A., 2012a. MPC 79224, 10.
 Tudorica, A., 2012b. MPC 79789, 7.
 Tudorica, A., 2012c. MPC 80000, 10.
 Tudorica, A., 2012d. MPC 77273, 5.
 Tudorica, A., 2012e. MPC 79533, 4.
 Tudorica, A., Badescu, T., 2011. MPC 76874, 4.
 Tudorica, A., Badescu, T., 2012. MPC 78902, 8.
 Tudorica, A., Toma, R., 2011. MPC 76451, 6.
 Vaduvescu, O., et al., 2008. *Planetary and Space Science* 56 (14), 1913.
 Vaduvescu, O., et al., 2011. *Planetary and Space Science* 59 (13), 1632.
 Vaduvescu, O., et al., 2012a. MPC 79787, 2.
 Vaduvescu, O., et al., 2012b. MPEC 2012-D82.
 Williams, G., private communication.
 Yoshida, F., et al., 2003. *Publications of the Astronomical Society of Japan* 55, 701.
 Yoshida, F., Nakamura, T., 2007. *Planetary and Space Science* 55, 1113.